J Chem Crystallogr (2011) 41:1418–1424
DOI 10.1007/s10870-011-0114-7

ORIGINAL PAPER

Crystal and Molecular Structures of 2-Amino-4-Nitrobenzoic Acid and Its Cocrystals with 2,2′-Bipyridine (2/1) and Bis(pyridin-2-yl)ketone (1/1)

James L. Wardell · Edward R. T. Tiekink

Received: 1 March 2011 / Accepted: 29 April 2011 / Published online: 12 May 2011

Abstract The eight-membered {···HOC=O}$_2$ synthon featured in the crystal structure of 2-amino-4-nitrobenzoic acid (**1**) is replaced by carboxylic acid···*N*-pyridine hydrogen bonds in its cocrystals with 2,2′-bipyridine (2/1; **2**) and bis(pyridin-2-yl)ketone (1/1; **3**) indicating the robust nature of the latter synthon. Disruption of the three-dimensional architecture based on O–H···O and N–H···O(nitro) hydrogen bonds in (**1**) is evident in the cocrystals which form supramolecular tubes (**2**) and chains (**3**) based on O–H···N and N–H···O hydrogen bonding. Compound (**1**) crystallizes in the monoclinic space group $P2_1/n$ with $a = 3.6291(1)$ Å, $b = 7.7339(3)$ Å, $c = 26.561(1)$ Å, $\beta = 91.385(2)°$, and $Z = 4$. Compound (**2**) crystallizes in the monoclinic space group $C2/c$ with $a = 27.562(3)$ Å, $b = 6.8300(6)$ Å, $c = 12.923(1)$ Å, $\beta = 110.593(5)°$, and $Z = 4$. Compound (**3**) crystallizes in the monoclinic space group $P2_1/c$ with $a = 3.795(3)$ Å, $b = 12.024(8)$ Å, $c = 35.65(2)$ Å, $\beta = 92.131(6)°$, and $Z = 4$ (determined from synchrotron data).

Keywords Carboxylic acid · Pyridines · Cocrystal · Hydrogen bonding · Supramolecular chemistry

Introduction

Investigations into the phenomenon of cocrystal formation, that is multicomponent crystals [1], are motivated by several imperatives. Primary amongst these are the applications in the pharmaceutical industry where the formation of a cocrystal represents a derivativation of the original drug by non-covalent association [2]. A key motivation behind cocrystal formation rests with the proposal that cocrystals formed with drugs have a reduced tendency to form polymorphs compared with the drugs themselves [3, 4], a consideration that has great implications for intellectual property issues. Additional impetus revolves practical concerns such an enhancing solubility for greater bio-availability, stability to humidity, prolonging shelf life, etc. [5, 6]. However, cocrystals have found uses predating these applications, such as in organic synthesis [7], for promoting crystal growth [8], as non linear optical materials [9], and for the separation of enantiomers [10]. Other perhaps less developed opportunities for cocrystals include their applications as luminescent materials [11], for stabilization of otherwise unstable chemical species [12], including volatile compounds such as perfumes [13], and for absolute structure determination [14].

In a sense, the formation of a cocrystal goes against the widely used technique of fractional crystallization for the purification of organic compounds. The formation of a cocrystal implies the resultant multicomponent crystal features preferable supramolecular synthons compared to those existing in the pure forms of the cocrystal formers. These ideas lead to the concept of a hierarchy of supramolecular synthons where synthons are listed in order of propensity of formation [15, 16], following on from the ideas of Etter [17]. Amongst the most reliable supramolecular synthons in crystal engineering of cocrystals and

J. L. Wardell (✉)
Centro de Desenvolvimento Tecnológico em Saúde (CDTS), Fundação Oswaldo Cruz (FIOCRUZ), Casa Amarela, Campus de Manguinhos, Av. Brasil 4365, Rio de Janeiro, RJ 21040-900, Brazil
e-mail: j.wardell@abdn.ac.uk

E. R. T. Tiekink (✉)
Department of Chemistry, University of Malaya, Kuala Lumpur 50603, Malaysia
e-mail: Edward.Tiekink@gmail.com

relevant to present study is that featuring a carboxylic acid-OH hydrogen bonded to a pyridyl-N atom [18]. In continuation of ongoing studies of cocrystal formation involving pyridyl-N atoms [19–23], in the present report, the crystal and molecular structures of 2-amino-4-nitrobenzoic acid, hitherto not described crystallographically, and its 2/1 and 1/1 cocrystals with the pyridine containing bases 2,2′-bipyridine and bis(pyridin-2-yl)ketone, respectively.

Experimental

Synthesis

Reagents were Commercial Samples. Crystals of 2-amino-4-nitrobenzoic acid were isolated from the slow evaporation from its ethanol solution; M.pt. 270–271 °C.

2-Amino-4-nitrobenzoic acid 2,2′-bipyridine (2/1)

A solution containing 2-amino-4-nitrobenzoic acid (1.0 mmol) and 2,2′-bipyridine (2.10 mmol) in ethanol (20 mL) was maintained at room temperature and crystals of the 2:1 cocrystalline product were slowly formed and harvested; M.pt. 197–198 °C.

A solution of 2-amino-4-nitrobenzoic acid (1.0 mmol) and 2,2′-bipyridine (1.1 mmol) in ethanol (20 mL) also gave crystals of the 2/1 cocrystal.

2-Amino-4-nitrobenzoic acid bis(pyridin-2-yl)ketone (1/1)

A solution containing 2-amino-4-nitrobenzoic acid (1.0 mmol) and bis(pyridin-2-yl)ketone (1.05 mmol) in ethanol (20 mL) was maintained at room temperature and crystals of the 1/1 cocrystalline product were slowly formed and harvested; M.pt. 185–188 °C.

In both cases the IR (in KBr) and ^{1}H NMR (in Me_2CO) spectra of the respective cocrystalline product were simple the summation of the spectra of the components as is often observed for cocrystals [19, 20, 23].

X-ray Crystallography

Intensity data for a bronze needle of (**1**) and an orange block of (**2**) were collected at 120 K on a Enraf–Nonius FR591 rotating anode CCD fitted with Mo Kα radiation. The data sets were corrected for absorption based on multiple scans [24] and reduced using standard methods [25, 26]. Data for a red rod of (**3**) were collected at 120 K on a Bruker SMART APEX2 CCD using synchrotron radiation with $\lambda = 0.6905$ Å; data processing was with CrystalClear [27] and APEX2 [28]. The structures were solved by direct methods with SHELXS-97 [29] and refined by a full-matrix least-squares procedure on F^2 using SHELXL-97 [29] with anisotropic displacement parameters for non-hydrogen atoms and a weighting scheme of the form $w = 1/[\sigma^2(F_o^2) + aP^2 + bP]$ where $P = (F_o^2 + 2F_c^2)/3$. Carbon-bound hydrogen atoms were included in the final refinement in their calculated positions with C–H = 0.95 Å. The acidic hydrogen atoms were located in difference Fourier maps and refined with O–H = 0.84(1) Å and N–H = 0.88(1) Å, and with $U_{iso}(H) = yU_{eq}$(parent atom); $y = 1.5$ for O and 1.2 for N. Disorder in the nitro group in (**1**) could not be resolved so in the final cycles of refinement the anisotropic displacement parameters were constrained to be nearly isotropic with the ISOR command in SHELXL-97 [29] and the N–O bond distances were refined with N–O = 1.220(1) Å. Crystal data and refinement details are given in Table 1. Figures 1, 2 and 3 showing the atom labeling schemes, were drawn with 50% displacement ellipsoids using ORTEP-3 [30], and the remaining figures were drawn with DIAMOND [31] with arbitrary spheres. Data manipulation and interpretation were accomplished using WinGX [32] and PLATON [33].

Results and Discussion

Molecular Structures

The molecular structure of the acid 2-amino-4-nitrobenzoic acid, (**1**), is shown in Fig. 1 and selected geometric parameters for this structure, as well as for (**2**) and (**3**), are displayed in Table 2. The molecule exists as the acid, a conclusion confirmed by the disparity in the C–O bond distances associated with the carboxylic acid residue, Table 2. The carboxylic acid is effectively coplanar with the aromatic ring to which it is connected, a configuration assured owing to the presence of an intramolecular N–H···O hydrogen bond formed between the proximate amino acid and the carbonyl-O2 atom. By contrast, the nitro group is twisted out of the plane, Table 2.

The asymmetric unit of (**2**) comprises a molecule of 2-amino-4-nitrobenzoic acid in a general position and half a 2,2′-bipyridine, as this is located about a crystallographic 2-fold axis, Fig. 2. Therefore, (**2**) is a 2/1 cocrystal. Confirmation of the presence of an acid is found in the derived geometric parameters which match closely those determined for the acid (**1**). By contrast to the situation in (**1**), both the carboxylic acid and nitro groups are coplanar with the aromatic ring, Table 2. There is a significant twist about the central C12–C12^i bond in the 2,2′-bipyridine molecule as seen in the value of the N3–C12–C12^i–N3^i torsion angle of 157.41(17)°; symmetry operation

Table 1 Crystal data and refinement details for (**1**)–(**3**)

Compound	(**1**)	(**2**)	(**3**)
Empirical formula	$C_7H_6N_2O_4$	$C_{10}H_8N_2$, $2(C_7H_6N_2O_4)$	$C_{11}H_5N_2O$, $C_7H_9N_2O_4$
Formula weight	182.14	520.46	366.33
Crystal habit, color	Needle, bronze	Block, orange	Rod, red
Crystal system	Monoclinic	Monoclinic	Monoclinic
Space group	$P2_1/n$	$C2/c$	$P2_1/c$
a (Å)	3.6291(1)	27.562(3)	3.795(3)
b (Å)	7.7339(3)	6.8300(6)	12.024(8)
c (Å)	26.561(1)	12.923(1)	35.65(2)
β (°)	93.569(2)	110.593(5)	92.131(6)
Volume (Å^3)	744.03(5)	2277.4(4)	1625.5(18)
Z	4	4	4
Density (calculated, g cm^{-3})	1.626	1.518	1.497
Absorption coefficient (mm^{-1})	0.136	0.117	0.112
$F(000)$	376	1080	760
Crystal size (mm)	0.05 × 0.05 × 0.25	0.11 × 0.20 × 0.40	0.005 × 0.005 × 0.06
θ range for data collection (°)	3.1–26.5	3.1–27.5	1.1–25.0
Reflections collected	14326	21394	12895
Independent reflections	1547	2613	3050
R_{int}	0.051	0.067	0.060
Reflections with $I \geq 2\sigma(I)$	1272	1909	2413
Number of parameters	127	181	253
Goodness-of-fit on F^2	1.07	1.04	1.09
Final R indices [$I \geq 2\sigma(I)$]	$R1 = 0.042$, $wR2 = 0.112$	$R1 = 0.055$, $wR2 = 0.136$	$R1 = 0.052$, $wR2 = 0.124$
a, b for weighting scheme	0.073, 0.159	0.093, 0.487	0.070, 0.403
R indices [all data]	$R1 = 0.051$, $wR2 = 0.119$	$R1 = 0.082$, $wR2 = 0.151$	$R1 = 0.068$, $wR2 = 0.137$
Largest difference peak and hole (Å^{-3})	0.32, −0.39	0.29, −0.32	0.35, −0.28
CCDC deposition no.	814981	814982	814983

$i = 1 - x, y, -1/2 - z$. The N atoms are orientated in opposite directions, a conformation that allows each to participate in significant hydrogen bonding interactions (see below). Cocrystal (**2**) was also isolated from the cocrystallization experiment containing equimolar quantities of the reagents highlighting the stability of the carboxylic acid···pyridine interaction.

The asymmetric unit of (**3**) comprises a single molecule each of 2-amino-4-nitrobenzoic acid and bis(pyridin-2-yl)ketone, Fig. 3, and is therefore a 1/1 cocrystal. Geometric parameters associated with the carboxylic acid reside match those found in (**1**) as does the coplanarity and twisting of the carboxylic acid and nitro groups, respectively, out of the plane of the aromatic ring. In the base, the dihedral angle between the pyridyl rings is 43.24(9)° indicating a significant twist in the molecule. As with (**2**), the N atoms are orientated in opposite directions to optimize hydrogen bonding interactions (see below). The hydrogen bond formed between the amino-H and the carbonyl-O5 brings into proximity one of the pyridine (N3) atoms resulting in a bifurcated interaction which effectively blocks off this site from interacting with the carboxylic acid. Hence, the isolation of the 1/1 cocrystal in contrast to the 2/1 cocrystal formed in the case when the base was 2,2′-bipyridine from the 1:1 cocrystallization experiment (see Experimental).

Supramolecular Aggregation

Based on O–H···O and N–H···O(nitro) hydrogen bonding, a three-dimensional architecture is apparent in the crystal structure of (**1**); see Table 3 for geometric data describing the most significant intermolecular forces operating in the crystal structures of (**1**)–(**3**). Centrosymmetrically related carboxylic acid residues associate via O–H···O hydrogen bonds to form an eight-membered {···HOC=O}$_2$ synthon. The dimeric aggregates are connected by N–H···O(nitro) hydrogen bonds whereby each amino-H forms a connection to a nitro-O of different molecules resulting in supramolecular chains extending in the *ab* plane; as the amino-

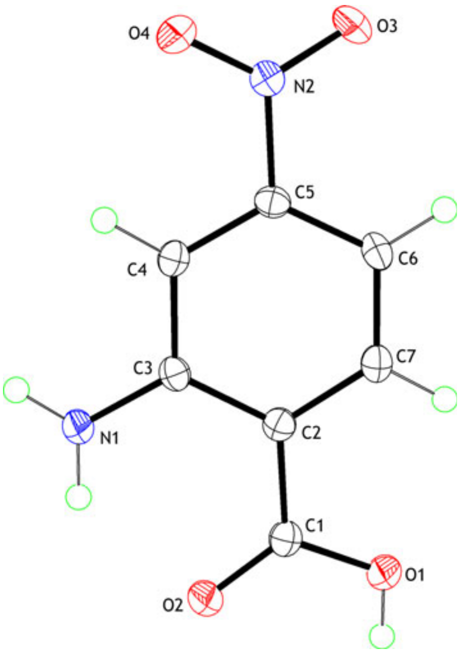

Fig. 1 The molecular structure of (**1**) showing atom labeling. Displacement ellipsoids are drawn at the 50% probability level (Color figure online)

Table 2 Selected bond lengths (Å), angles (°), and torsion angles (°) for the 2-amino-4-nitrobenzoic acid molecule in (**1**)–(**3**)

Parameter	(**1**)	(**2**)	(**3**)
C1–O1	1.324(2)	1.331(2)	1.346(3)
C1–O2	1.238(2)	1.222(2)	1.238(2)
C1–C2	1.469(2)	1.486(2)	1.495(3)
C3–N1	1.347(2)	1.354(2)	1.371(3)
O1–C1–O2	121.8(1)	122.8(2)	122.1(2)
C2–C1–O1	114.7(1)	113.7(1)	113.5(2)
C2–C1–O2	123.5(1)	123.5(2)	124.4(2)
O1–C1–C2–C3	175.9(1)	−173.6(1)	−179.0(2)
C4–C5–N2–O3	−165.4(1)	−177.3(2)	164.7(2)

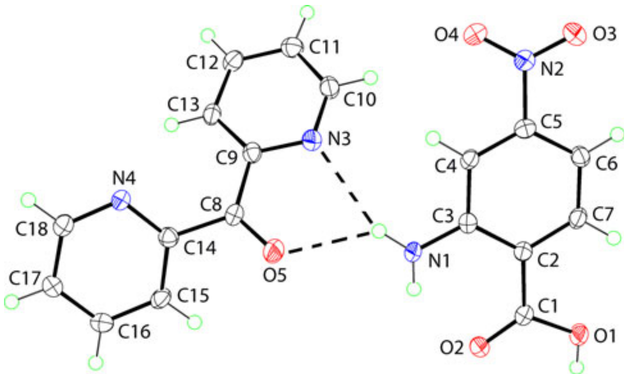

Fig. 3 The two molecular aggregate of (**3**) showing atom labeling. Hydrogen bonds are shown as *dashed lines*. Displacement ellipsoids are drawn at the 50% probability level (Color figure online)

H1*n* atom also forms an intramolecular N–H···O2 contact, it is bifurcated (Fig. 4).

In (**2**), the familiar carboxylic acid dimer is absent as the carboxylic acid-OH forms a hydrogen bond with the pyridyl-N3 atom, an arrangement stabilized by a close C–H18···O2 contact resulting in the seven membered {HOC=O···HCN} heterosynthon [18]. By contrast to that found in (**1**), the amino-H atoms form hydrogen bonds with carboxylic acid-O rather than nitro-O atoms with each H atom forming a contact to one of the O atoms of the former; the persistence of the intramolecular H1*n*···O2 hydrogen bond is noted. The result of the hydrogen bonding is the formation of supramolecular tubes aligned along the *c* axis, Fig. 5a, b. The tubes are connected into the three-dimensional structure via C–H···O interactions involving the nitro-O atoms, Fig. 6.

As with (**2**), the carboxylic acid-OH forms a hydrogen bond with a pyridyl-N4 atom; a close C–H8···O2 contact closes the seven membered {HOC=O···HCN} heterosynthon. The amino-H atoms participate into three hydrogen bonding contacts. As with the previous structures, the H1*n* atom forms an intramolecular hydrogen bond with the carboxylic acid-O2 atom. The H2*n* atom is bifurcated,

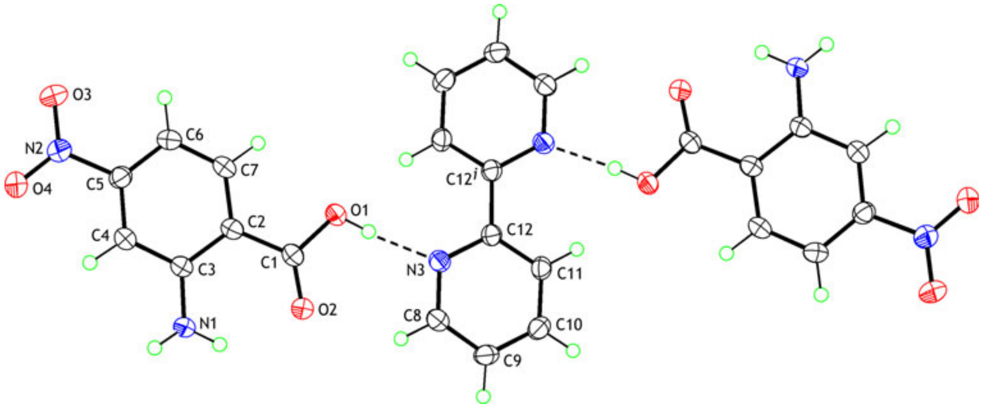

Fig. 2 The three molecular aggregate of (**2**) showing atom labeling for the asymmetric unit; symmetry operation *i*: $1 - x$, y, $-1/2 - z$. Hydrogen bonds are shown as *dashed lines*. Displacement ellipsoids are drawn at the 50% probability level (Color figure online)

Table 3 Hydrogen bonding parameters (A–H···B; Å, °) for (**1**)–(**3**)

A	H	B	H···B	A···B	A–H···B	Symmetry operation
(**1**)						
O1	H1*o*	O2	1.80(2)	2.653(2)	178(1)	$2 - x, -y, -z$
N1	H1*n*	O2	2.04(2)	2.688(2)	130(1)	x, y, z
N1	H1*n*	O3	2.45(2)	2.820(2)	106(1)	$1 + x, -1 + y, z$
N1	H2*n*	O4	2.25(1)	3.093(2)	161(1)	$2\frac{1}{2} - x, -1/2 + y, 1/2 - z$
(**2**)						
O1	H1*o*	N3	1.81(2)	2.664(2)	176(2)	x, y, z
N1	H1*n*	O2	2.04(2)	2.697(2)	131(1)	x, y, z
N1	H1*n*	O2	2.49(2)	3.088(2)	125(1)	$1 - x, y, 1/2 - z$
N1	H2*n*	O1	2.24(2)	3.076(2)	159(2)	$x, 1 - y, 1/2 + z$
C8	H8	O2	2.40	3.157(2)	137	x, y, z
C9	H9	O3	2.57	3.465(3)	157	$-1/2 + x, 1\frac{1}{2} - y, -1/2 + z$
C10	H10	O4	2.46	3.405(2)	176	$-1/2 + x, 1/2 + y, -1 + z$
(**3**)						
O1	H1*o*	N4	1.98(2)	2.814(3)	170(2)	$x, 1 + y, z$
N1	H1*n*	O2	2.07(2)	2.769(3)	136(2)	x, y, z
N1	H2*n*	O5	2.38(2)	3.091(3)	138(2)	x, y, z
N1	H2*n*	N3	2.55(2)	3.367(4)	155(2)	x, y, z
C18	H18	O2	2.49	3.273(4)	140	$x, -1 + y, z$
C13	H13	O1	2.53	3.353(4)	146	$-1 + x, -1 + y, z$
C16	H16	O2	2.55	3.443(4)	156	$-1 - x, -1/2 + y, 1/2 - z$

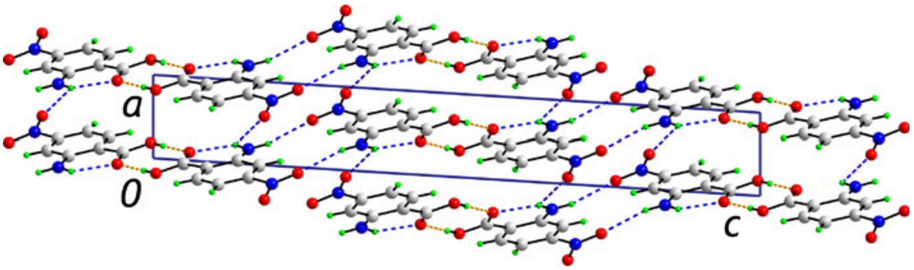

Fig. 4 View in projection down the *b* axis of the crystal packing in (**1**). The O–H···O and N–H···O hydrogen bonds are shown as *orange and blue dashed lines*, respectively (Color figure online)

being connected to the carbonyl-O5 and pyridyl-N3 atoms. The result is the formation of a supramolecular chain along the *b* axis, Fig. 7. Interactions of the type C–H···O involving the carboxylic acid-O atoms exclusively link chains into layers two molecules thick that stack along *c*, Fig. 8. The nitro groups lie to the periphery of the layers, resembling the situation seen for (**2**), and form weaker C–H···O contacts but longer the standard criteria in PLATON [33]. The shortest of these contacts involves C6–H6 and $O3^i$ [$H6\cdots O3^i = 2.62$ Å, $C6\cdots O3^i = 3.444$ (3) Å with an angle at $H6 = 145°$ for $i: 2 - x, 1 - y, 1 - z$].

Conclusions

The presence of 2-amino-4-nitrobenzoic acid in its cocrystals formed with 2,2′-bipyridine (2/1) and bis(pyridin-2-yl)ketone (1/1) is confirmed by comparison of geometric parameters defining the respective carboxylic acid residues. The characterization of cocrystals presented herein represents the first reported for 2-amino-4-nitrobenzoic acid which has hitherto only been characterized in its salts according to a search of the CSD [34]. There are three examples of salts, namely ethylenediammonium 4-nitroanthranilate dehydrate [35], dicyclohexylammonium 4-nitroanthranilate [36], and guanidinium 2-amino-4-nitrobenzoate monohydrate [37]. In each of these the original base did not feature a pyridine-N atom and proton transfer occurred during the cocrystallisation experiment. The isolation of the cocrystals (**2**) and (**3**) is a testament to the robust nature of the seven-membered carboxylic acid···*N*-pyridine synthon [18].

Supplementary Material

CCDC 814981–814983 contains the supplementary crystallographic data for the three structures reported in this

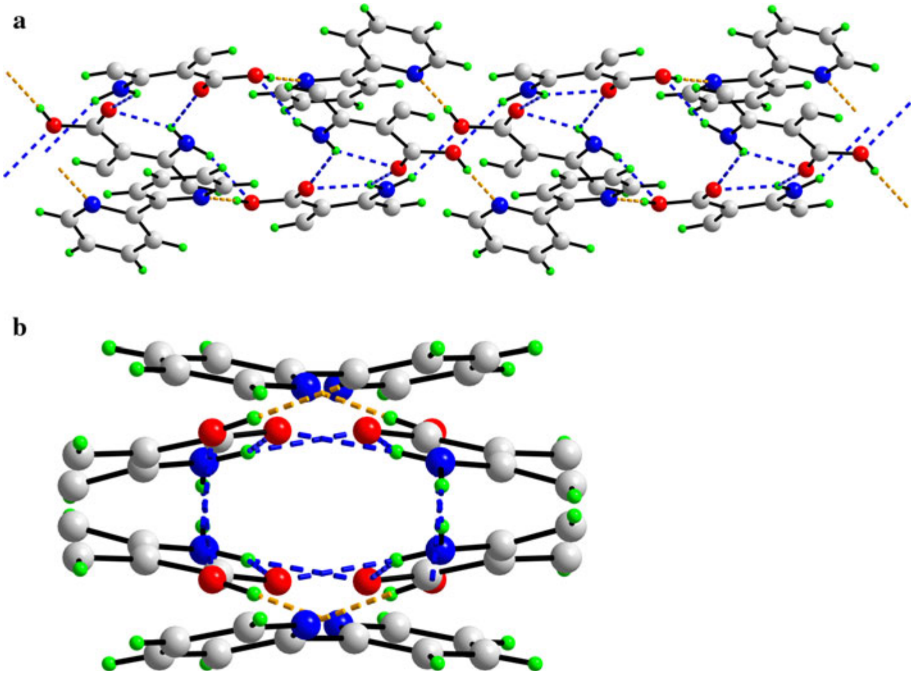

Fig. 5 Supramolecular tube in (**2**) sustained by O–H···O and N–H···O hydrogen bonds shown as *orange and blue dashed lines*, respectively: **a** side-on view and **b** end-on view (Color figure online)

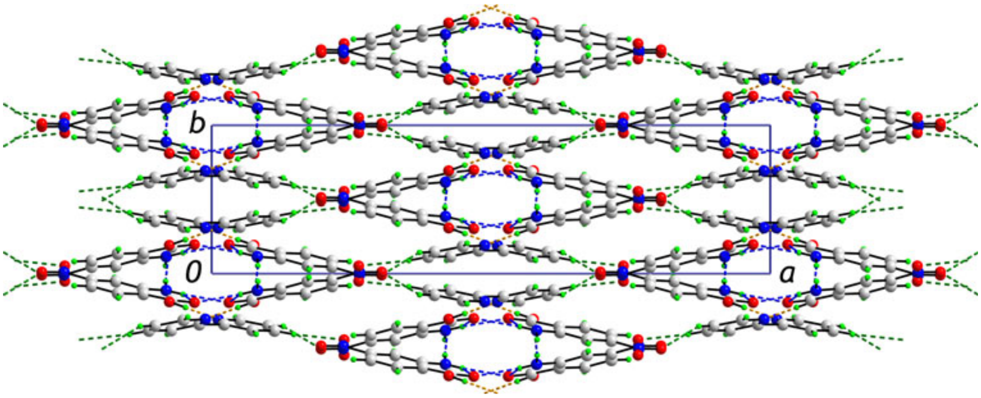

Fig. 6 View in projection down the *c* axis of the crystal packing in (**2**). The O–H···O and N–H···O hydrogen bonds, and C–H···O contacts are shown as *orange*, *blue* and *green dashed lines*, respectively. The supramolecular tubes, shown in Fig. 5, are orientated in the *c* direction and are connected by C–H···O contacts (Color figure online)

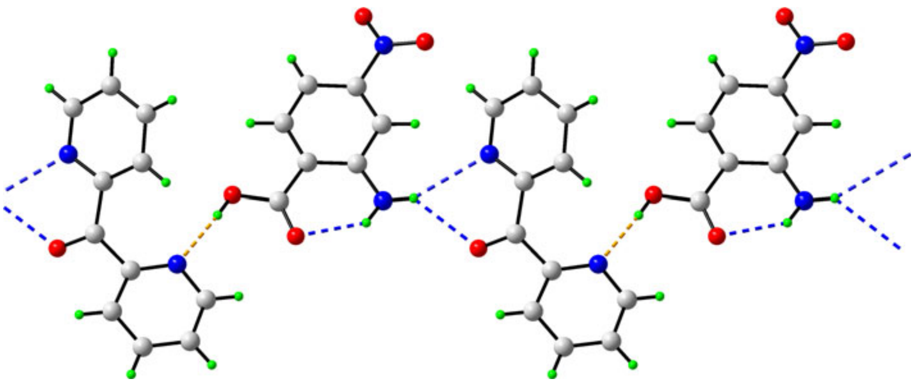

Fig. 7 Supramolecular chain aligned along *b* in (**3**) with a flat topology and sustained by O–H···O and N–H···O hydrogen bonds shown as *orange and blue dashed lines*, respectively (Color figure online)

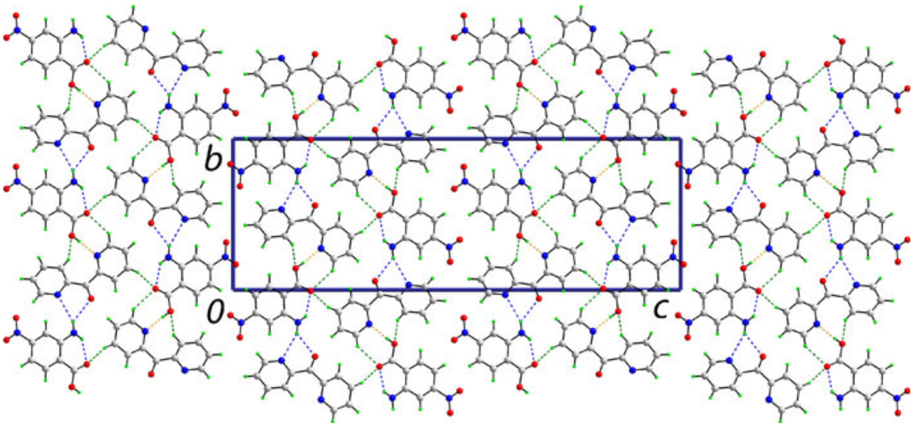

Fig. 8 A view of the unit cell contents in (**3**) shown in projection down the *a* axis highlighting the stacking of layers along *c*. The O–H···O and N–H···O hydrogen bonds, and C–H···O contacts are shown as *orange*, *blue* and *green dashed lines*, respectively (Color figure online)

paper. These data can be obtained free of charge at www.ccdc.cam.ac.uk/conts/retrieving.html [or from the Cambridge Crystallographic Data Centre (CCDC), 12 Union Road, Cambridge CB2 1EZ, UK; fax +44(0)1223-336033; email: deposit@ccdc.ccam.ac.uk].

Acknowledgments JLW acknowledges support from CAPES and FAPEMIG (Brazil). The University of Malaya is thanked for support this research (UMRG RG125/10AFR). The use of the EPSRC X-ray crystallographic service at the University of Southampton, England, Prof. W. Clegg and the synchrotron component, based at Daresbury, and the valuable assistance of the staff at those centers are gratefully acknowledged.

References

1. Zukerman-Schpector J, Tiekink ERT (2008) Z Kristallogr 223:233
2. Weyna DR, Shattock T, Reddy V, Zaworotko MJ (2008) Cryst Growth Des 8:4533
3. Morissette SL, Soukasene S, Levinson D, Cima MJ, Almarsson Ö (2003) Proc Natl Acad Sci USA 100:2180
4. Arora KK, Zaworotko MJ (2009) In: Brittain HG (ed) Polymorphism in pharmaceutical solids, vol 2. Informa Healthcare, New York
5. Good DJ, Rodríguez-Hornedo N (2009) Cryst Growth Des 9:2252
6. Schultheiss N, Newman A (2009) Cryst Growth Des 9:2950
7. Gao X, Friščić T, MacGillivray LR (2004) Angew Chem Int Ed 43:232
8. Etter MC, Baures PW (1988) J Am Chem Soc 111:639
9. Huang K-S, Britton D, Etter MC, Byrn SR (1997) J Mater Chem 7:713
10. Hoekstra MS, Sobieray DM, Schwindt MA, Mulhern TA, Grote TM, Huckabee BK, Hendrickson VS, Franklin LC, Granger EJ, Karrick GL (1997) Org Process Res Dev 1:26
11. Hori A, Takatani S, Miyamoto TK, Hasegawa M (2009) CrystEngComm 11:567
12. Han J, Zang S-Q, Mak TCW (2010) Chem Eur J 16:5078
13. Iimura N, Fujimura Y, Sekine A, Kitagawa S, Ohashi Y (2005) Bull Chem Soc Jpn 78:418
14. Bhatt PM, Desiraju GR (2008) CrystEngComm 10:1747
15. Almarsson Ö, Zaworotko MJ (2004) Chem Commun 1889
16. Bis JA, Vishweshwar P, Weyna DR, Zaworotko MJ (2007) Mol Pharmacol 4:401
17. Etter MC (1990) Acc Chem Res 23:120
18. Shattock TR, Arora KK, Vishweshwar P, Zaworotko MJ (2008) Cryst Growth Des 8:4533
19. Broker GA, Tiekink ERT (2007) CrystEngComm 9:1096
20. Broker GA, Bettens RPA, Tiekink ERT (2008) CrystEngComm 10:879
21. Kaiser CR, Pais KC, de Souza MVN, Wardell JL, Wardell SMSV, Tiekink ERT (2009) CrystEngComm 11:1133
22. Corlette EM, Tiekink ERT (2009) J Chem Crystallogr 39:603
23. Ellis CA, Miller MA, Spencer J, Zukerman-Schpector J, Tiekink ERT (2009) CrystEngComm 11:1352
24. Sheldrick GM (2007) SADABS. University of Göttingen, Germany
25. Hooft RWW (1998) COLLECT data collection software. Nonius B.V., Delft
26. Otwinowski Z, Minor W (1997) In: Carter CW Jr, Sweet RM (eds) Methods in enzymology, vol 276, Macromolecular crystallography, Part A. Academic Press, New York, pp 307–326
27. Rigaku MSC (2008) CrystalClear. Rigaku/MSC Inc., The Woodlands
28. Bruker (2008) Bruker AXS Inc., Madison
29. Sheldrick GM (2008) Acta Crystalogr A64:211
30. Farrugia LJ (1997) J Appl Crystallogr 30:565
31. Brandenburg K (2006) DIAMOND, Version 3.1c. Crystal Impact GbR, Bonn
32. Farrugia LJ (1999) J Appl Crystallogr 32:827
33. Spek AL (2009) Acta Crystallogr D65:148
34. Allen FH (2002) Acta Crystallogr B58:380
35. Smith G, Wermuth UD, White JM (2002) Acta Crystallogr E58:o1088
36. Smith G, Wermuth UD, Healy PC (2004) Acta Crystallogr E60:o684
37. Smith G, Wermuth UD, Healy PC, White JM (2007) Acta Crystallogr E63:o7